Current Chemistry Letters 12 (2023) 623–640

Contents lists available at GrowingScience

Current Chemistry Letters

homepage: www.GrowingScience.com

Synthesis and evaluation of green magnetic mesoporous molecularly imprinted polymers for adsorption removal of parabens from cosmetic samples

Nursyahera Azreen Ramin[a] and Saliza Asman[a*]

[a]*Department of Physics and Chemistry, Faculty of Applied Sciences and Technology, Universiti Tun Hussein Onn Malaysia (UTHM), Malaysia*

C H R O N I C L E

Article history:
Received September 28, 2022
Received in revised form
December 25, 2022
Accepted January 27, 2023
Available online
January 27, 2023

Keywords:
Green magnetic nanoparticles
Deep eutectic solvent
Molecularly imprinted polymer
Mesoporous
Adsorption behavior
Cosmetic samples

A B S T R A C T

Parabens are chemicals that are frequently used as preservatives in numerous cosmetic products. In recent years, the safety concern over these compounds has grown due to their endocrine-disrupting activity. In this research, a novel green magnetic molecularly imprinted polymer (GMMIP) was synthesised using propylparaben as a template and then applied as an adsorbent to selectively recognise and remove parabens from cosmetic samples. The green strategies were introduced by using *Persicaria odorata* or *Kesum* leaf extract as a reducing agent to synthesise green magnetic nanoparticles (MNP) as a magnetic core, and deep eutectic solvent (DES) has been designed as an environmentally friendly functional monomer that was used in the preparation of GMMIP. The GMMIP was characterised using Fourier transform infrared spectroscopy (FTIR), field emission scanning electron microscopy (FESEM), and Brunauer-Emmett-Teller (BET). The results of FESEM and BET indicated that the GMMIP exhibited an irregular spherical shape and mesoporous characteristics with a pore size of 17.74 nm. The adsorption pH, kinetics, isotherms, and thermodynamics parameters were performed to investigate the interactions that take place between GMMIP and propylparaben. The adsorption processes appeared to best fit the pseudo-second-order kinetic and Freundlich isotherm models at an optimum pH of 12. Findings from a thermodynamics study revealed the adsorption process was exothermic, spontaneous, and more favourable at 298 K. The optimised GMMIP was applied as an adsorbent to remove the parabens from cosmetic samples. When compared to methylparaben and ethylparaben, the GMMIP had the highest selectivity and effectively removed propylparaben, with recoveries ranging from 75.6% to 113.3%. It was found that the limits of detection (LOD) and quantification (LOQ) were between 0.03 and 0.05 mg/L and 0.11 and 0.16 mg/L, respectively. The synthesised GMMIP proved to be a convenient and effective adsorbent to remove parabens from cosmetic products.

1. Introduction

Currently, parabens are one of the most used preservatives in cosmetic products such as shampoos, lotions, deodorants, scrubs, sunscreens, and eye make-up[1]. However, parabens are included in a long list of compounds that are either forbidden or controlled and have an impact on the safety of cosmetics. For preservation, a mixture of two or three types of parabens is usually employed. However, recent research has indicated that parabens are classified as an "endocrine-disrupting chemical" (EDC) since they can harm both human and animal health by disturbing the endocrine system[2]. Another study revealed that paraben exposure can harm the reproductive system[3]. Additionally, it has been established that parabens may cause breast cancer[4].

* Corresponding author.
E-mail address salizaa@uthm.edu.my (S. Asman)

doi: 10.5267/j.ccl.2023.1.008

According to the European Union (EU) Council Directive and the National Pharmaceutical Regulative Agency (NPRA) of Malaysia, parabens are permitted in cosmetic products in maximum amounts of 0.4% as a single usage and 0.8% for the overall number of parabens in the cosmetic products[5]. Nowadays, there are many "paraben-free" cosmetics on the market, and consumers have generally reacted well to them. However, labelling fraud is made easier by the lack of legislation. It is currently becoming more and more crucial to control the presence of parabens in cosmetics, even those marketed as "paraben-free," to ensure consumer safety[6]. Numerous separation techniques, including solid-phase extraction (SPE), solid-phase microextraction (SPME), dispersive liquid-liquid microextraction (DLLME), and ultrasonic-assisted extraction (UAE), have been developed. However, several of these techniques have limitations, including being time-consuming, laborious, and using a lot of hazardous solvents[7]. Therefore, preconcentration methods are crucial methods implemented for sample preparation prior to the separation techniques mentioned above.

Molecularly imprinted polymers (MIPs) have recently evolved into a promising material for the preconcentration, identification, and removal of several types of molecules. Molecularly imprinted polymer (MIP) is a synthetic polymer created by introducing the target molecule (template) and then removing it with an appropriate solvent[8]. As a result, the unique cavities obtained are matched to the target molecule in terms of functional group, size, and structure[9]. MIPs can detect and bind the template molecule given by the presence of imprinted cavities, making it possible to separate and detect the template molecule[10]. MIPs have numerous benefits, including ease of production, good stability, and a relatively low cost[11]. Nevertheless, traditional MIPs have a few drawbacks, such as incomplete template removal, slow binding rates, and the fact that some of the reagents employed to produce MIP are harmful[12].

The contribution of the green magnetic nanoparticles (MNP) approach has provided many advantages for molecular imprinting technology (MIT), which can improve some of the fundamental characteristics of MIP[13]. Recently, the green synthesis of magnetic nanoparticles by biological methods has gained a lot of interest since it has significant benefits over chemical and physical methods, including being easy to prepare, cost-effective, and producing less waste[14]. For example, magnetite nanoparticles Fe_3O_4 have emerged as a potential candidate for study among all magnetic nanoparticles because of their superparamagnetic characteristics, biocompatibility, and low toxicity[15]. There have been numerous reports of successful studies employing different plant extracts for MNP synthesis, such as *Zanthoxylum armatum* DC[16], *Dolichos lablab* L[17], *Kappaphycus alvarezii*[18], *Calliandra haematocephala*[19], and *Lagenaria siceraria*[20]. Fortunately, no research has yet described the use of *Persicaria odorata* extract to manufacture MNP.

Persicaria odorata (Polygonum odoratum), locally known as "*Kesum*" in Malaysia, is an edible plant that belongs to the *Polygonaceae* family and the Persicaria genus[21]. In addition to its culinary usage as a flavouring ingredient, this plant is also used in traditional medicine as an anti-diabetic, antioxidant, antibacterial, anti-inflammatory, anti-stress, and anti-cancer agent[22, 23]. It has been suggested that proteins, amino acids, organic acids, vitamins, as well as secondary metabolites like flavonoids, alkaloids, polyphenols, terpenoids, heterocyclic compounds, and polysaccharides that are present in plants play an important role in metal salt reduction as well as act as capping and stabilising agents to synthesise the nanoparticles [24, 25].

Meanwhile, there has been an increase in interest in employing deep eutectic solvent (DES) as a green functional monomer in the synthesis of MIPs[26, 27]. DES has numerous advantages, including a wide range of polarity, low volatility and toxicity, water-miscibility, and biodegradability. By altering the hydrogen bond donor or acceptor, a specific DES can be created, which improves the specific identification of MIP in contrast to traditional MIP. Numerous studies have demonstrated that using a specifically designed DES as a functional monomer in the MIP polymerization process can enhance the selectivity and affinity of the target molecules[28]. Therefore, the main goal of this work is to synthesise and apply green magnetic molecularly imprinted polymer (GMMIP) as an adsorbent for the removal of parabens from cosmetic samples. The parabens were determined and quantified using UV-VIS analysis. The green MNP was first synthesised using *Kesum* leaf extract as a reducing agent via the co-precipitation method for the first time in a straightforward and environmentally beneficial manner. The MNP was then used as the magnetic core in the synthesis of GMMIP. Besides that, the designed DES was also introduced as an eco-friendly functional monomer to accomplish the green aspect of the GMMIP synthesis. The characteristics and adsorption performance of GMMIP were also investigated. To our knowledge, this study marks the first attempt to use *Kesum* leaf extract and DES for the synthesis of MIPs dedicated to paraben removal from cosmetic samples.

2. Experimental

2.1 Materials

Iron (II) chloride tetrahydrate ($FeCl_2.4H_2O$, 99%) and Iron (III) chloride hexahydrate ($FeCl_3.6H_2O$, 99%) were supplied by R&M Chemicals whereas ammonia solution (NH_4OH, 25%) and toluene ($C_6H_5CH_3$) were supplied by Merck. Moreover, tetraethyl orthosilicate (TEOS, $C_8H_{20}O_4Si$, 98%), (3-Aminopropyl) triethoxysilane (APTES, $C_9H_{23}NO_3Si$, 99%), choline chloride (ChCl, $C_5H_{14}CINO$, 98%) propyl 4-hydroxybenzoate (propylparaben, $C_{10}H_{12}O_3$ 99%), methyl 4-hydroxybenzoate

(methylparaben, $C_8H_8O_3$, 99%), ethyl 4-hydroxybenzoate (ethylparaben, $C_9H_{10}O_3$, 99%), methacrylic acid (MAA, $C_4H_6O_2$, 99%), trimethylolpropane trimethacrylate (TRIM, $C_{15}H_{20}O_6$), and benzoyl peroxide (BPO, $C_{14}H_{10}O_4$) were supplied by Sigma-Aldrich. Methanol (CH_3OH, 99%) and acetic acid ($C_2H_4O_2$, 96%) were supplied by Fisher Scientific. Meanwhile, ethanol (C_2H_5OH 95%) was supplied by HmbG Chemicals. The deionized water was commercially available from our laboratory.

2.2 Preparation of plant extract (Kesum leaf extract)

5 g of *Kesum* leaves were bought from a supermarket in Muar, Johor, Malaysia (latitude: 2° 2' 45.5784" N; longitude: 102° 34' 4.3644" E). The leaves were first rinsed with tap water and then with deionized water to get rid of any dust. The leaves were then cut into smaller pieces and boiled in 100 ml of deionized water for 2 hours at 80 °C until the colour of the aqueous solution changed to a golden yellow. The extract was filtered onto filter paper and stored at a temperature of 4 °C for later use[29].

2.3 Synthesis of green magnetic nanoparticles (MNP)

The green MNP was synthesised following the[30] method with a slight modification via the co-precipitation method using *Kesum* leaf extract as a reducing agent. The metal salts Fe^{3+} ($FeCl_3.6H_2O$, 1.1 g) and Fe^{2+} ($FeCl_2.4H_2O$, 0.5 g) were put into a three-necked round bottom flask that was filled with 100 ml of deionized water. The reaction was allowed to run for 1 hour at 80 °C with constant stirring and in the presence of nitrogen. Then, 5 ml of the *Kesum* leaf extract was gradually added to the reaction mixture. The reaction mixture was then adjusted to pH 10 by adding NH_4OH dropwise. The final product (black precipitate) was rinsed with deionized water several times and once with ethanol. The product was then subjected to a 24-hour vacuum drying process at 60 °C.

2.4 Modification and functionalization of magnetic nanoparticles surfaces (MNP@SiO_2-NH_2)

The green MNP was modified with SiO_2 following the[31, 32] methods in the following procedures: About 0.3 g of MNP was mixed with 50 ml of ethanol and 4 ml of ultrapure water before being ultrasonically processed for 15 minutes. Then, 5 ml of NH_4OH and 2 ml of TEOS were added and stirred for 12 hours at room temperature. The final product (MNP@SiO_2) was obtained and rinsed with ethanol and water before being dried at 60 °C in a vacuum. Next, the MNP@SiO_2 nanoparticles were functionalized using APTES as follows: 2 g of MNP@SiO_2 nanoparticles and 50 ml of toluene were ultrasonically mixed for 15 minutes in a three-necked flask. The mixture was then treated with 4 ml of APTES and refluxed at 110 °C for 12 hours with constant stirring while being protected by nitrogen gas. The product obtained (MNP@SiO_2-NH_2) was isolated by filtering, repeatedly rinsed with ethanol, and dried for 12 hours at 60 °C under vacuum.

2.5 Synthesis of deep eutectic solvent (DES)

The deep eutectic solvent (DES) was prepared following the[33] method using choline chloride and methacrylic acid (ChCl/MAA) in a beaker with a 1:2 molar ratio. The mixture was stirred on a hot plate at 80 °C until a uniform liquid was produced. After being cooled to room temperature, the DES was employed as a green functional monomer in the GMMIP synthesis.

2.6 Synthesis of green magnetic molecularly imprinted polymer (GMMIP)

The GMMIP was synthesised via the precipitation polymerization method. About 0.2 mmol (0.036 g) of the template (propylparaben) was dissolved in 20 ml of methanol, and then 1 ml of the DES (functional monomer) was added. The mixture was stirred for 30 minutes to form the template-monomer complex. Next, about 0.1 g of MNP@SiO_2-NH_2, 4.0 mmol (1.23 ml) of the trimethylolpropane trimethacrylate, TRIM (cross-linker), and 0.05 g of benzoyl peroxide, BPO (initiator) were introduced to the present mixture solution and ultrasonically mixed for 15 minutes. The reaction mixtures were stirred at 87 °C for 24 hours after being nitrogen-purged for 10 minutes. Finally, a magnet was used to collect the produced GMMIP, and the template was then removed with a 9:1 methanol-acetic acid wash. The templates were totally eluted until the eluent was propylparaben-free by UV-VIS spectrophotometer detection[34, 35]. The same technique was used to produce the green magnetic non-imprinted polymer (GMNIP), but without propylparaben. The proposed polymerization process for GMMIP is given in **Fig. S1.**

2.7 Characterization

Several instruments were used to characterise the synthesised materials in the preparation of the GMMIP. FTIR spectra were recorded using Perkin-Elmer. All the samples were run between 400 and 4000 cm^{-1}. Field emission scanning electron microscopy (FESEM, FEI Versa 3D Dual Beam) was used to examine the appearance of each sample in order to examine

the morphology and surface structure of the materials. The surface area and porous characteristics of the materials were assessed using the Brunauer-Emmett-Teller (BET) method (Sorptometric 1990 Series, USA). The quantification of propyl-, ethyl-, and methylparaben was performed at λ_{max} = 256 nm using a UV-VIS spectrophotometer (Shimadzu UV 3600, Japan)

2.8 Batch adsorption studies

2.8.1 Preliminary batch study

The performances of the produced adsorbents (MNP, GMMIP, and GMNIP) were compared by adsorption experiments. The temperature was set to 25 °C, the analyte solution was 10 ml, the sorbent dosage was 10 mg, and the contact time was 1 hour at 100 rpm. After adsorption, a magnet was used to separate the adsorbent, and the eluent was then filtered before being analysed with a UV-VIS spectrophotometer with a maximum 256 nm wavelength[36]. The adsorption capacity (mg/g) and removal efficiency (%) of each sample were calculated in triplicate using Eq. (1) and Eq. (2), as shown below:

$$\text{Adsorption capacity (mg/g)} = \frac{(C_o - C_e)}{W} \times V \quad (1)$$

$$\text{Removal efficiency (\%)} = \frac{C_o - C_e}{C_o} \times 100 \quad (2)$$

where C_o and C_e are the concentration of target compound solution before and after adsorption (mg/L) respectively, V is the solution volume (L) and W is the polymer mass (g)[37].

2.8.2 Effect of pH

The adsorption capacity of propylparaben was investigated in various pH solutions while keeping other variables constant. The pH of 10 ml of a 10 mg/L propylparaben solution containing 10 mg of GMMIP was studied in the range of 1-13. Sodium hydroxide (NaOH, 0.1 M) or hydrochloride acid (HCl, 0.1 M) were added to the solution in the necessary amounts to control the pH. At room temperature, the mixture was mechanically shaken for an hour. The propylparaben concentration was measured both before and after adsorption, and the adsorption capacities of the GMMIP were calculated [38].

2.8.3 Effect of contact time

10 mg of GMMIP was weighed and suspended in 10 ml of a 10 mg/L propylparaben solution. The mixture was shaken mechanically for 0-90 minutes at room temperature. The propylparaben concentration was measured both before and after adsorption, and the adsorption capacities of GMMIP were calculated[39].

2.8. Effect of initial concentrations

10 mg of the GMMIP was added to a centrifuge tube with 10 ml of paraben solution at various concentrations (10, 20, 30, 40, 50, and 60 mg/L). The mixture was shaken mechanically at room temperature for the optimum contact time. The initial and final concentrations of propylparabens were determined to calculate the adsorption capacities[39].

2.8.5 Effect of adsorption thermodynamics

10 mg of GMMIP was placed in a centrifuge tube that contained 10 ml of a 10 mg/L propylparaben solution. The mixture was shaken mechanically at optimum contact time at different temperatures using a mechanical shaker and was centrifuged at 100 rpm. The adsorption capacities of GMMIP were calculated[39].

2.9 Application of GMMIP for removal of parabens from cosmetic samples

2.9.1 Sample preparation

The cosmetic samples were purchased at a local store in Muar, Johor, and included body wash, deodorant, face cleanser, moisturizer, lotion, and toner. The cosmetic samples were diluted with deionized water at a 1:100 dilution ratio, filtered through a 0.45 µm membrane filter to eliminate contaminants, and stored in the dark at 4 °C [40].

2.9.2 Removal of parabens in cosmetic samples

The efficiency of GMMIP to remove parabens from cosmetic samples was tested following the[36, 41] method with slight modifications. The recovery experiment was carried out using the cosmetic samples that were spiked with parabens (methylparaben, ethylparaben, and propylparaben) at a concentration level of 1 mg/L. A centrifuge tube was filled with 10 mg of GMMIP. After that, 10 ml of the spiked cosmetic samples were added, and it was shaken for 15 minutes. A permanent magnet was then used to collect the GMMIP, which was subsequently rinsed with 3 ml of water. Finally, the parabens (propylparaben, ethylparaben, and methylparaben) were eluted from GMMIP using 10 ml of methanol/acetic acid solution

(99:1, v/v) after 15 minutes of shaking. A 0.45 µm membrane filter was used to filter the elute, which was then subjected to UV-VIS spectrophotometry analysis.

3. Result and discussion

3.1 Characterization of green magnetic molecularly imprinted polymer

3.1.1 Functional group analysis

The FTIR spectra of *Kesum* leaf extract, MNP, MNP@SiO_2, MNP@SiO_2-NH_2, GMMIP, and GMNIP are displayed in **Fig. 1**. Initially, the green MNP was synthesised using *Kesum* leaf extract as a reducing agent. **Fig. 1 (a)** shows the FTIR spectrum of the extract of *Kesum* leaf. It showed distinctive bands at 1634 cm^{-1} and 3318 cm^{-1}, respectively, which denoted the presence of the C=O group of carboxylic acid and the O-H group of phenolic compounds. The presence of the obvious Fe-O peak at 543 cm^{-1}, as shown in **Fig. 1 (b)**, indicates that green MNP was successfully synthesised. The characteristic band due to the O-H group of phenol was found to be shifted from 3318 cm^{-1} to 3217 cm^{-1}, which is indicative that it functions as a reducing agent in the production of green MNP. The band associated with the C=O group of carboxylic acid was slightly shifted from 1634 cm^{-1} to 1633 cm^{-1} compared to the aqueous extract of *Kesum* leaf. The presence of a peak at 1434 cm^{-1} was due to the C=C group of aromatic compounds[16, 42]. In **Fig. 1 (c)**, for MNP@SiO_2, there were four strong peaks observed. The strong peaks at 1067 cm^{-1} and 795 cm^{-1} could be assigned to the asymmetric and symmetric stretching vibrations of Si-O-Si bonding, while the peaks at 447 cm^{-1} and 954 cm^{-1} were associated with the bending vibrations of Si-O-Si and Si-OH, respectively. It has been established that a silica layer was grafted onto the surface of MNP[43]. In **Fig. 1 (d)**, for the MNP@SiO_2-NH_2, the presence of a peak at 1636 cm^{-1} was caused by the vibration of N-H, which indicates that APTES was successfully applied on magnetic nanoparticle surfaces. The absorption band of C=O in TRIM was seen at 1722 cm^{-1} and 1724 cm^{-1} for GMMIP and GMNIP, respectively, in **Fig. 1 (e)** and **Fig. 1 (f)**. The outcomes demonstrated that the materials were developed favourably and that MNP@SiO_2-NH_2 surfaces had successfully been grafted with a polymer layer[44, 45].

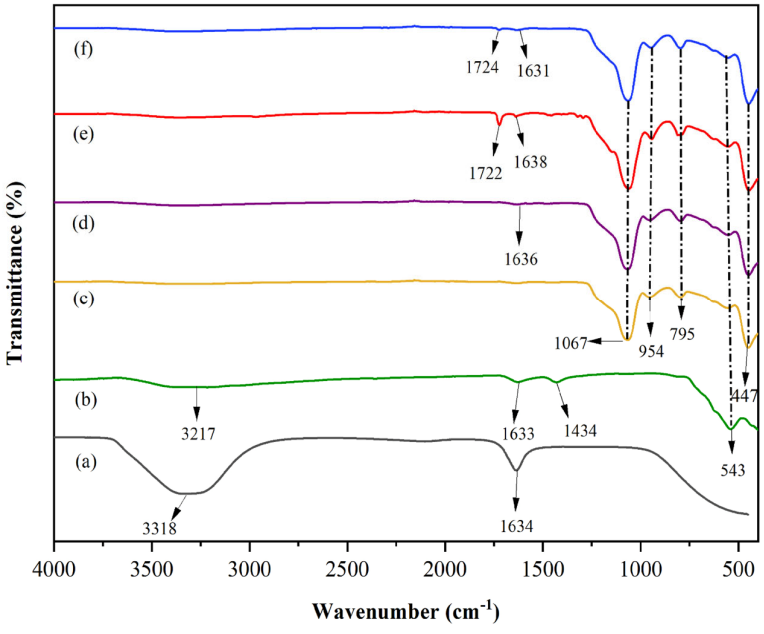

Fig. 1. FTIR spectra of (a) *Kesum* leaf extract (b) MNP, (c) MNP@SiO_2, (d) MNP@SiO_2-NH_2, (e) GMMIP, and (f) GMNIP.

3.1.2 Morphological and particle size analysis

Fig. 2 depicts the results of a FESEM analysis of the surface morphology, structure, and particle size of MNP, MNP@SiO_2, MNP@SiO_2-NH_2, GMMIP, and GMNIP. For morphological investigation, the relevant particle size distribution histogram was produced using Image-J software and given in **Fig. S2**. After Gaussian fitting to the histograms provided by Origin software, the average particle size of the data was obtained. As illustrated in **Fig. 2 (a)**, the produced green magnetic nanoparticles, MNP, had an irregular spherical form and agglomerated with an average diameter of 98.19 nm. As a result of being coated with a silica layer and going through APTES functionalization, MNP@SiO_2 (**Fig. 2 (b)**) and MNP@SiO_2-NH_2 (**Fig. 2 (c)**) gradually increased in size. The sizes of MNP@SiO_2 and MNP@SiO_2-NH_2 are substantially bigger and smoother in shape, with average diameters of 205.35 nm and 209.15 nm, respectively. After polymerization, the surface morphology of GMMIP (**Fig. 2 (d)**) and GMNIP (**Fig. 2 (e)**) was reported to have more rough

surfaces, with average diameters of 243.70 nm and 252.35 nm, respectively. The incremental change resulted in a rise in the size of the materials, suggesting that the modification and polymerization processes were successful[46].

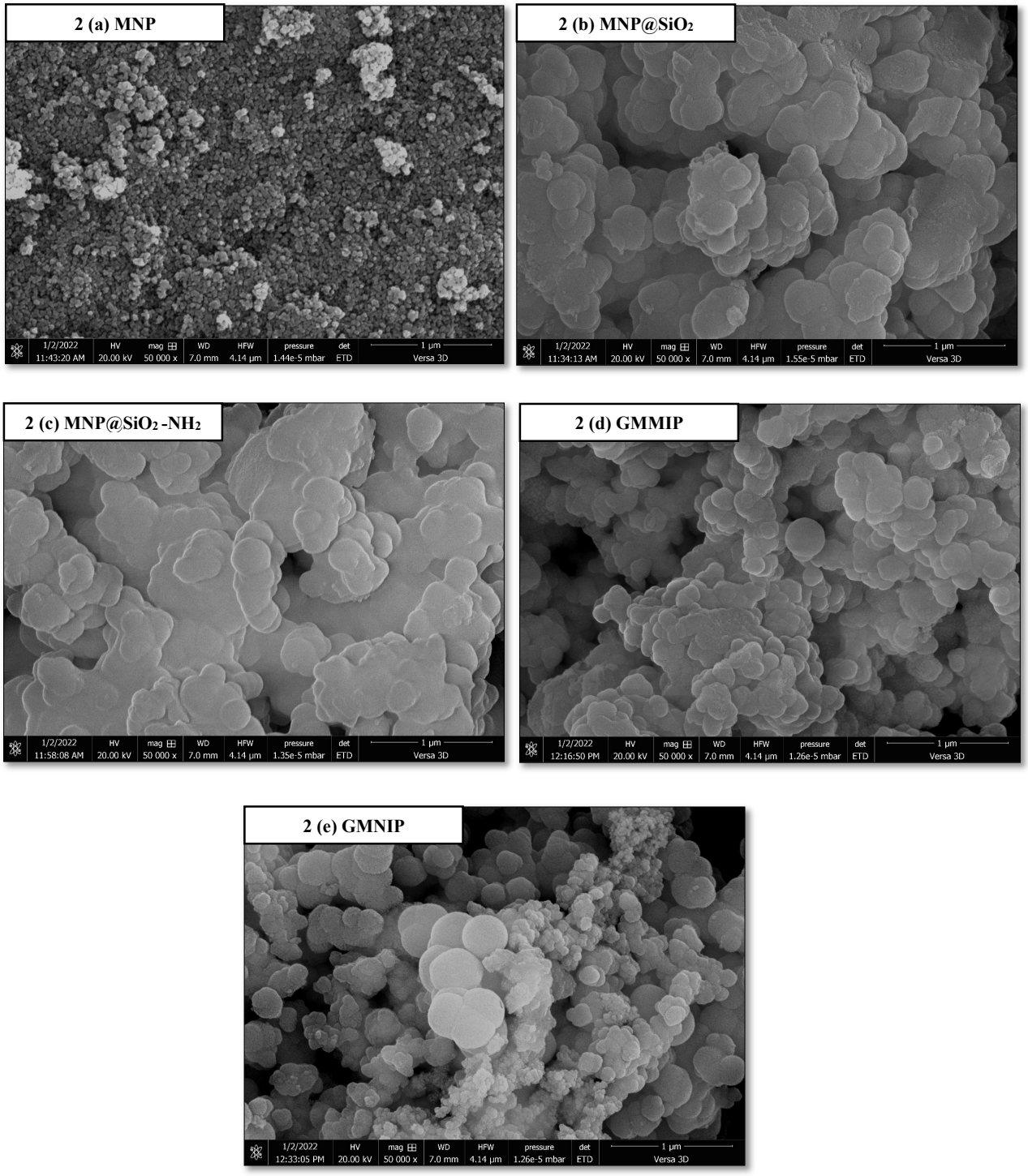

Fig. 2. The FESEM images of (a) MNP, (b) MNP@SiO_2 (c) MNP@SiO_2-NH_2, (d) GMMIP, and (e) GMNIP.

3.1.3 Surface area analysis

The porosity and specific surface area of the three synthesised adsorbents, MNP, GMMIP, and GMNIP, were determined using Brunauer-Emmet-Teller (BET) as given in **Table 1**. **Fig. 3** shows the findings of nitrogen adsorption and desorption of MNP, GMMIP, and GMNIP. The surface areas of MNP, GMMIP, and GMNIP were 85.87 $m^2 g^{-1}$, 5.02 $m^2 g^{-1}$, and 4.52 $m^2 g^{-1}$, respectively. The surface area of bare MNP decreased, which indicated modification and polymerization had taken

place. These three adsorbents have average pore sizes of 10.39 nm for MNP, 17.74 nm for GMMIP, and 15.25 nm for GMNIP. Among the three adsorbents, the GMMIP has the largest pores, which can offer a template for better adsorption. Additionally, type IV isotherms were seen in the adsorption isotherms of all the adsorbents, indicating the presence of mesoporous and capillary condensation[47]. Mesoporous materials (2–50 nm) contain pores that are between those of microporous (2 nm) and macroporous (> 50 nm). Mesoporous materials have greater benefits than microporous and macroporous materials, including a large surface area, a large pore volume, and strong stability[48]. The MNP displayed typical type IV isotherms with H1-type hysteresis loops ascribed to cylindrical or columnar pores. The adsorption and desorption curves are parallel, and the two curves are perpendicular to the pressure axis at the narrow region, indicating that the distribution of pore diameter is narrowing[49]. Meanwhile, the GMMIP and GMNIP had H4-type hysteresis loops owing to slit-shaped pores. This wide hysteresis loop and the steeper desorption curve than the adsorption curve suggest that the materials may have different pore types and pore diameter distributions[50].

Table 1. Summary of BET analyses for MNP, GMMIP, and GMNIP.

Type of analysis	MNP	GMMIP	GMNIP
Surface area (m^2 g^{-1})	85.87	5.02	4.52
Pore volume (cm^3 g^{-1})	0.240	0.006	0.004
Pore size (nm)	10.39	17.74	15.25
N^2 adsorption / desorption isotherm	Type IV isotherm with H1-type hysteresis loop	Type IV isotherm with H4-type hysteresis loop	Type IV isotherm with H4-type hysteresis loop

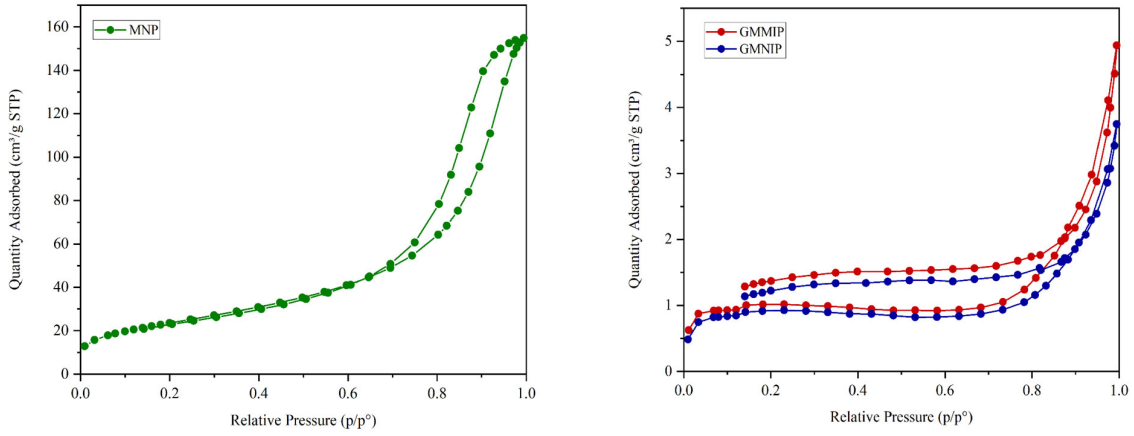

Fig. 3. BET data of nitrogen adsorption / desorption isotherms of MNP, GMMIP, and GMNIP.

3.2 Optimization performance of GMMIP for paraben adsorption

3.2.1 Preliminary batch study

A preliminary study was carried out on three synthesised materials (MNP, GMMIP, and GMNIP) to investigate their performances against propylparaben, as shown in **Fig. S3**. The results showed that the GMMIP (0.9523 mg/g) has the best adsorption capacity, followed by the MNP (0.6694 mg/g), and the GMNIP (0.3375 mg/g) has the lowest capacity towards the propylparaben. The adsorption capacity is influenced by the differences in particle morphology, particle size, and pore area of the materials. The results imply a considerable improvement in adsorption for GMMIP compared to MNP and GMNIP, since the main goal of this study is to improve and increase the selectivity of the MIP features. Following a comparison of the types of these three adsorbents, GMMIP and MNP were chosen for further adsorption studies. Several aspects impacting performance, such as the effect of pH, kinetics, isotherms, and thermodynamics adsorption, were explored to assess the capability of the GMMIP for the removal and determination of parabens in cosmetic samples.

3.2.2 Effect of pH

The effect of pH on the adsorption capacity was studied over a pH range of 1–13. From **Fig. 4**, the adsorption capacity of propylparaben showed similar trends from pH 1 to pH 13 for both MNP and GMMIP. The results demonstrated that the adsorption capacity of propylparaben by both MNP and GMMIP declined from pH 1 to pH 3 and subsequently increased from pH 4 to pH 12. However, as it reaches pH 13, the readings drop. The optimal pH for both MNP and GMMIP was discovered to be pH 12. Propylparaben is protonated below pH 3, hence its binding capacity is limited. Parabens are mostly neutral at pH 3–6.5[51]. Parabens occur predominantly in a negatively charged form at pH values ranging from 7 to 12 because the hydroxyl group has now been entirely deprotonated. The binding capacity rises considerably in this area, reaching a peak at pH 12. This is because when propylparaben is deprotonated, it forms hydrogen bonds and electrostatic interactions

with MNP and GMMIP[52, 53]. However, when the pH is raised to pH 13, the binding capacity is reduced once again. This is because paraben molecules are completely converted into alcohol and hydroxybenzoic acid[51]. As a result of this optimization, pH 12 appeared to be the most favourable condition for future adsorption studies.

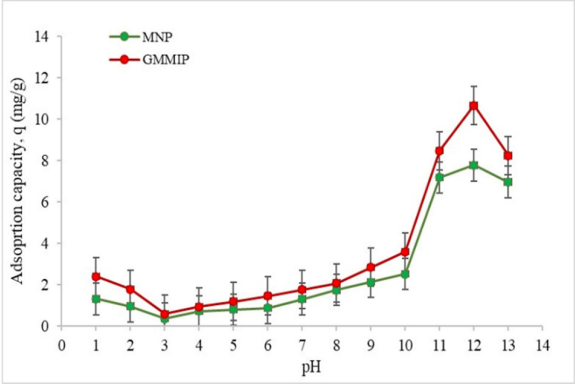

Fig. 4. Effect of pH on propylparaben adsorption by MNP and GMMIP.

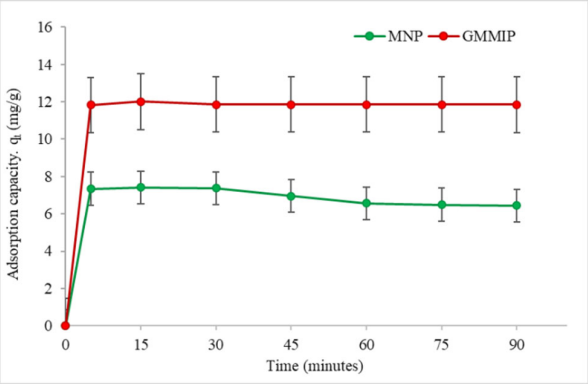

Fig. 5. Effect of contact time on propylparaben adsorption by MNP and GMMIP.

3.2.3 Effect of contact time

The effect of contact time on propylparaben adsorption and removal using the MNP and GMMIP was studied within the intervals of 0-90 minutes at room temperature. The findings are represented in **Fig. 5** and **Fig. 6**, respectively. The adsorption capacity shows a rapid increase during the first 15 minutes, owing to the availability of active sites for both adsorbents, MNP and GMMIP. It was found that the adsorption rate had gradually flattened after 15 minutes. This may be because more propylparaben molecules had saturated the mesoporous at this moment than during the first 15 minutes of adsorption. Since then, the propylparaben molecules have been pushed further and deeper into the pores, facing considerably more resistance, causing the adsorption to slow down[54]. In addition, the availability of recognition sites on GMMIP is thought to be the reason why the adsorption capacity of GMMIP is clearly greater than that of MNP. As a result, 15 minutes was shown to be the optimum contact time for both adsorbents, with removal efficiencies of 73.19 % (MNP) and 80.75 % (GMMIP), indicating their ability to effectively bind and remove the propylparaben. Therefore, 15 minutes was chosen as the equilibrium point for the studied parabens throughout the investigation.

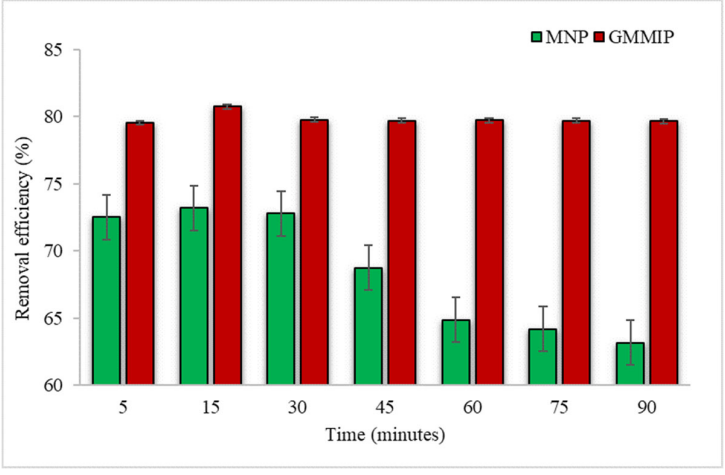

Fig. 6. Effect of contact time on propylparaben removal by MNP and GMMIP.

3.2.4 Adsorption kinetics

The adsorption kinetics data based on the contact time study were analysed using the pseudo-first-order model (**Fig. S4**) and the pseudo-second-order model (**Fig. S5**) to better understand how the propylparaben and the adsorbents interact. The slope ($-k_1/2.303$) and intercept ($\log q_e$) of the linear curve $\log (q_e - q_t)$ vs t in Eq. (3) can be used to calculate the values of q_e and k_1 for the pseudo-first-order model. The values of q_e and k_2 for the pseudo-second order model can be found from the linear curve of t/q_t versus t with intercept ($1/k_2q_e^2$) and slope ($1/q_e$) in Eq. (4).

Pseudo-first-order model:

$$\log (q_e - q_t) = \log q_e - \frac{k_1 t}{2.303} \quad (3)$$

Pseudo-second-order model:

$$\frac{t}{q_t} = \frac{1}{k_2 q_e^2} + \left(\frac{1}{q}\right) t \quad (4)$$

where q_e and q_t are the adsorbed amounts at equilibrium and time t (mg/g), t is the time (min), and k_1 is the pseudo-first-order rate constant (min^{-1}). The value of k_1 is obtained by plotting log (q_e-q_t) versus t. The rate constant is always inversely proportional to the initial solute concentration, although some research has found that k_1 increases with or without the initial solute concentration. This is because, for a higher initial solute concentration, a longer time is needed[55, 56]. In order to describe the validity and suitability of the adsorption kinetics, the normalized standard deviation Δq (%) and relative error (%) were calculated using Eq. (5) and Eq. (6), respectively[36]. The kinetic parameters for the adsorption of MNP and GMMIP to propylparaben are summarized in **Table 2**.

Normalized standard deviation:

$$\Delta q\ (\%) = \sqrt{\frac{\left(\frac{q_{exp}-q_{cal}}{q_{exp}}\right)^2}{N-1}} \times 100 \quad (5)$$

Relative error (%)

$$\text{Relative error } (\%) = \frac{\left|q_{exp}-q_{cal}\right|}{q_{exp}} \quad (6)$$

where N is the number of data points, whereas q_{exp} and q_{cal} (mg/g) are the experimental and calculated adsorption capacities, respectively.

Table 2. Kinetic parameters for the propylparaben adsorption of MNP and GMMIP.

Parameters of kinetic model	Adsorbent	
	MNP	GMMIP
$q_{e,exp}$ (mg/g)	7.4073	12.0008
Pseudo-first-order kinetic model (PFO)		
$q_{e,cal}$ (mg/g)	3.9683	5.2155
k_1 (min^{-1})	0.0221	0.0493
Δq (%)	32.83	39.98
Relative error (%)	46.43	56.54
R^2	0.5173	0.7589
Pseudo-second-order kinetic model (PSO)		
$q_{e,cal}$ (mg/g)	5.8997	11.2994
k_2 (min^{-1})	0.0208	0.0076
Δq (%)	14.39	4.13
Relative error (%)	20.35	5.84
R^2	0.9990	0.9965

It is evident that the regression coefficient (R^2) that was produced from linear curves of pseudo-second-order for MNP (R^2 = 0.9990) and GMMIP (R^2 = 0.9965) was greater than that for MNP (R^2 = 0.5173) and GMMIP (R^2 = 0.7589) obtained from pseudo-first-order. Moreover, the experimental adsorption capacity, $q_{e,exp}$ (MNP = 7.4073 mg/g and GMMIP = 12.008 mg/g) obtained was close to the calculated adsorption capacity, $q_{e,cal}$ (MNP = 5.8997 mg/g and GMMIP = 11.2994 mg/g) that was obtained from the pseudo-second-order model, whereas the calculated adsorption capacity, $q_{e,cal}$ obtained from the pseudo-first order model for MNP and GMMIP was 3.9683 mg/g and 5.2155 mg/g, respectively. The high regression coefficient (R^2), the similarity between the experimental and calculated adsorption capacities, and the lower Δq values of 14.39 % (MNP) and 4.13 % (GMMIP), with relative error (%) of 20.35 % (MNP) and 5.84 % (GMMIP), suggested that the pseudo-second-order model was more precise to represent the kinetic adsorption of propylparaben onto MNP and GMMIP than the pseudo-first-order model.

If the experimental data fit with the pseudo-first-order model, the adsorption was followed by physisorption, in which boundary-layer diffusion occurs. Meanwhile, the pseudo-second-order model proposed chemisorption as the rate-limiting step between the interaction of adsorbent and analytes. Therefore, it is proposed that the rate-limiting step for the adsorption of propylparaben on MNP and GMMIP may be chemisorption. However, several researchers argue that adsorption processes cannot be correctly attributed solely to kinetic investigations or the use of kinetic models alone. To determine whether adsorption is a chemical or physical process, many analytical techniques, including FTIR, Raman spectroscopy, and TGA, must be used in conjunction with information on the activation and adsorption energies of the molecules and

adsorptive thermodynamic data[57]. Due to this, the thermodynamic investigation was continued in this work in order to confirm the types of adsorptions involved.

3.2.5 Effect of initial concentrations

The effect of initial concentrations was studied using 10 mg of MNP / GMMIP at optimum pH 12 for 15 minutes at room temperature with various initial concentrations ranging from 10 to 60 mg/L. It is shown in **Fig. 7** that when the concentration increased, more propylparaben was adsorbed onto MNP / GMMIP. This happened because an increase in propylparaben concentration led to a reduction in the resistance to propylparaben absorption from the solution. Additionally, the rate of propylparaben adsorption also increases as the concentrations increase, which is associated with an increase in driving force[54]. Increasing driving force increases the likelihood of molecular collisions and the surface area of the adsorbent, which tends to increase mass transfer from the solution phase to the solid phase. **Fig. 8** illustrates the relationship between the initial concentration and the amount of propylparaben removed by MNP and GMMIP. The removal efficiency of propylparaben by MNP increased until it reached equilibrium at 30 mg/L with a removal efficiency of 81.2 %, whereas the removal efficiency of GMMIP achieved equilibrium at 50 mg/L with a removal efficiency of 81.4 %. Thus, the findings conclude that paraben saturation occurs at a particular concentration because there are only a finite number of active sites on the surface of the adsorbents[36].

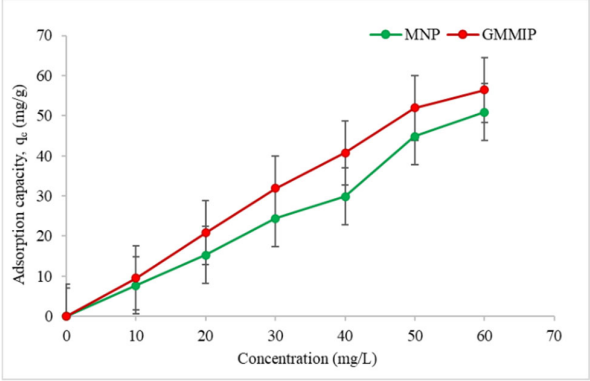

Fig. 7. Effect of initial concentration on propylparaben adsorption by MNP and GMMIP.

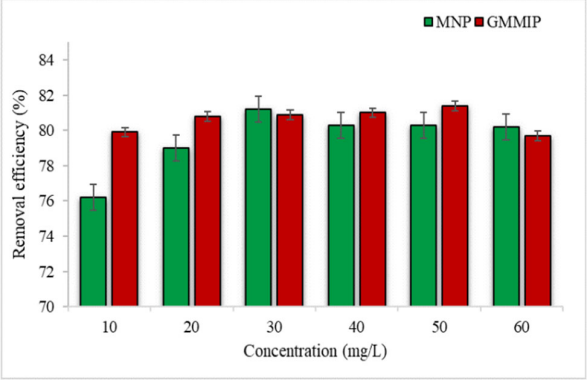

Fig. 8. Effect of initial concentration on propylparaben removal by MNP and GMMIP.

3.2.6 Adsorption isotherms

The adsorption isotherms model is crucial to describing how an adsorbate interacts with the adsorbent at constant temperature and pH. As a result, many isotherm models, such as the Langmuir model and the Freundlich model, have been proposed by researchers to produce an appropriate correlation for experimental data. The Langmuir equation is explained by Eq. (7) below:

$$\frac{c_e}{q_e} = \frac{1}{K_L q_m} + \frac{c_e}{q_m} \tag{7}$$

where c_e denotes the equilibrium adsorbate concentration (mg/L), q_e is the equilibrium adsorption capacity (mg/g), q_m is the maximum adsorption capacity (mg/g), and K_L represents the Langmuir constant (L/mg).

The Langmuir isothermal model has some limitations in that it assumes that the adsorption energy for a homogeneous adsorbent surface is identical for each site, contrary to the fact that an adsorbent has heterogeneous surfaces with different adsorption energies for each site[58]. The Langmuir constant, K_L, is correlated with adsorption capacity, where greater surface area and volume of pore can lead to greater adsorption capacity. Meanwhile, the basic characteristics of the Langmuir isotherm can be represented by the separation factor R_L. From Eq. (8) below, K_L and C_0 represent the Langmuir constant (mg/g) and initial concentration of adsorbate (mg/g), respectively. The R_L value shows the adsorption to be either linear ($R_L = 1$), irreversible ($R_L = 0$), unfavorable ($R_L > 1$), or favorable ($0 < R_L < 1$)[59].

$$R_L = \frac{1}{1 + K_L C_0} \tag{8}$$

Meanwhile, the heterogeneity and multilayer adsorption of molecules onto the adsorbent surfaces are identified using the Freundlich isotherm model[60]. The Freundlich isotherm model is illustrated by Eq. (9).

$$\log q_e = \log K_F + \frac{1}{n_F} \log c_e \quad (9)$$

where q_e (mg/g) is the number of molecules adsorbed to the adsorbent surface, c_e (mg/L) is the equilibrium concentration of adsorbate, K_F (mg/g) is the adsorption capacity of the adsorbent, and $1/n_F$ is the intensity of the adsorption.

Table 3. Isotherm parameters for the adsorption of MNP and GMMIP to propylparaben.

Parameters of isotherm model	Adsorbent	
	MNP	GMMIP
	Langmuir model	
q_m (mg/g)	103.09	94.34
K_L (L/mg)	0.0615	0.0985
R_L	0.35	0.16
R^2	0.1359	0.3292
	Freundlich model	
K_F ($mg^{(1-1/n)} L^{1/n}/g$)	3.6417	4.3631
n_F	1.0727	1.0287
$1/n_F$	0.9322	0.9721
R^2	0.9872	0.9966

In this study, the equilibrium data of the MNP and GMMIP adsorption processes were fitted using the Langmuir model (**Fig. S6**) and the Freundlich model (**Fig. S7**). The correlation coefficient (R^2) in linear regression is used to investigate the applicability of the isotherms model to adsorption behaviors. The R^2 value that is most closely related to 1 indicates that the isotherms model offers the best fit to the experimental data. The parameters of the isotherm model of MNP and GMMIP are represented in **Table 3**. The adsorption processes of MNP and GMMIP were assumed not to comply with the Langmuir model due to their R^2 values. The R^2 values of MNP and GMMIP from the Langmuir adsorption model were 0.1359 and 0.3292, respectively, which are very low. The Langmuir isotherm showed maximum adsorption capacities, $q_{m,}$ with values of 103.09 and 94.34 mg/g for MNP and GMMIP, respectively. Furthermore, the Langmuir constant, K_L value for GMMIP (K_L= 0.0985 L/mg) was higher than MNP (K_L= 0.0615 L/mg) which indicates the higher capacity and affinity of GMMIP than MNP. Moreover, the Langmuir model may be used to determine the R_L values, which show whether the adsorption process is preferred or not. The R_L values obtained for MNP and GMMIP were 0.35 and 0.15, respectively, which were in the range of $0 < R_L < 1$, demonstrating the favorable adsorption under the studied conditions. The Langmuir model makes the following assumptions: (1) that the surface is homogeneous, in which case all adsorption sites are energetically equivalent; (2) that adsorption occurs in a monolayer with each site only capable of adsorbing one adsorbate molecule; (3) that there is no lateral interaction between adsorbed molecules; and (4) that adsorption is reversible[61]. Thus, from all the results obtained, the propylparaben adsorption onto MNP and GMMIP was disregarded since the Langmuir model primarily applies to monolayer adsorption on a homogenous system.

Based on the R^2 values of the Freundlich isotherm model exceeding 0.95, which were 0.9872 for MNP and 0.9966 for GMMIP, this suggests that the adsorption of propylparaben on MNP and GMMIP was designed for heterogeneous systems and multilayer adsorption. In addition, the values of K_F and $1/n_F$ may be determined from the experimental data plotted from log q_e vs log c_e from Eq. (9) using the intercept and slope of the linear equation. The Freundlich adsorption capacity (K_F) indicates whether a system is favorable for adsorption. Adsorption appears promising when K_F is between 1 and 20[55], and the findings show that the K_F in this study was 3.6417 for MNP and 4.3631 for GMMIP. Besides that, the higher K_F value of GMMIP compared to MNP revealed that GMMIP had a better adsorption system and offered more heterogeneous binding sites than MNP. Similarly, $1/n_F$ denotes the strength of adsorption or surface heterogeneity, reflecting the energy-relative distribution and the heterogeneity of adsorbate sites. The fact that $1/n_F < 1$ for both MNP and GMMIP suggests that the adsorption process was favorable and that physisorption occurred as $n_F > 1$[36, 46]. Overall, the Freundlich isotherm model outperformed the Langmuir isotherm model at explaining the adsorption of propylparaben onto MNP and GMMIP.

3.2.7 Adsorption thermodynamics

Thermodynamic experiments were conducted to investigate how temperature affects the adsorption mechanism. Various thermodynamic parameters are calculated using Eq. (10) and Eq. (11), which are the key characteristics of the adsorption mechanism, such as enthalpy change (ΔH°), Gibbs free energy change (ΔG°), and entropy change (ΔS°). By measuring these thermodynamic parameters, the nature of the adsorption process can be predicted[48].

$$\ln K_d = \frac{\Delta S^\circ}{R} - \frac{\Delta H^\circ}{RT} \quad (10)$$

$$\Delta G^\circ = -RT \ln K_d \quad (11)$$

where T is the temperature (K), R is the gas constant, and the value K_d can be obtained from q_e/c_e. A linear plot should be generated by a plot of ln K_d versus 1/T (**Fig. S8**) and ΔH° and ΔS° can be calculated from the slope and intercept, respectively[62].

The adsorption enthalpy (H°), change of entropy (S°), and Gibbs free energy (G°) were calculated from the slope and intercept of a Van't Hoff plot of ln K_d vs 1/T using Eq. (10) to evaluate the thermodynamic feasibility of the propylparaben adsorption onto MNP/GMMIP. From **Table 4**, the negative value of ΔH° indicated an exothermic process for both adsorption systems, MNP and GMMIP. Being an exothermic process, sorption should be expected to become less effective as the temperature of the adsorbate-adsorbent system increases. It is also discovered that the ΔH° of GMMIP (-8.46 kJ/mol) was higher than the value of ΔH° of MNP (-8.84 kJ/mol). It could be because the adsorbate molecule interacts with the adsorbent surfaces in the GMMIP adsorption system more strongly than in the MNP adsorption system. The magnitude of the ΔH° which ranges from -2.1 to -20.9 kJ/mol, implies that physisorption has taken place[63]. The findings from the Freundlich isotherm model support this hypothesis. Furthermore, the values of ΔS° for MNP (-19.84 J/Kmol) and GMMIP (-14.64 J/Kmol) were also obtained. The negative values of ΔS° for both systems were correlated with the decrease in randomness at the solid/solution during sorption, indicating a more ordered transition state than the initial state[64]. ΔG° could serve as an indicator to verify the spontaneity of the adsorption process. The result demonstrated that a spontaneous process occurred in the adsorption system, as shown by the negative values of ΔG° for MNP and GMMIP. The spontaneous process implies that no external energy input was needed for the system. In addition, a more negative ΔG° value indicates a stronger driving force for adsorption, which enhances the capacity for adsorption. Propylparaben adsorption was clearly demonstrated to be more favourable and have greater adsorptive affinity on GMMIP compared to MNP due to the more negative value of ΔG° of GMMIP. As the temperature rises, the absolute ΔG° values also seem to increase, which suggests that the conditions for propylparaben molecule adsorption are less favorable. Hence, it can be concluded that the adsorption of propylparaben on the MNP and GMMIP was observed to be physisorption, exothermic in nature, spontaneous, and more favorable at low temperatures.

Table 4. Thermodynamic parameters for propylparaben adsorption by MNP and GMMIP.

Adsorbent	Temperature (K)	Enthalpy ΔH° (kJ/mol)	Entropy ΔS° (J/Kmol)	Gibbs energy ΔG° (kJ/mol)
MNP	298	-8.84	-19.84	-2.89
	318			-2.62
	338			-2.09
GMMIP	298	-8.46	-14.64	-4.04
	318			-3.93
	338			-3.44

3.3 Application of GMMIP in real cosmetic samples

3.3.1 Method validation

A standard calibration with six different concentrations (0.1, 0.2, 0.4, 0.6, 0.8, and 1.0 mg/L) for all three parabens was plotted. The evaluation of the calibration curve, correlation coefficients (R^2), limit of detection (LOD), and limit of quantification (LOQ) for the method for the detection of parabens in cosmetic samples is given in **Table S1**. The linearity of calibration curves was discovered to be within the range of 0.1 to 1.0 mg/L, and the correlation coefficient was found to be between 0.9995 and 0.9998, indicating that the linear range of analytes has satisfactory linearity. Additionally, based on 3 and 10 times the signal-to-noise ratio (S/N), the values of LOD and LOQ were determined to be in the ranges of 0.03 to 0.05 mg/L and 0.11 to 0.16 mg/L, respectively.

3.3.2 Analysis of real samples

Under optimal conditions, the proposed method of magnetic molecular imprinting technique was used in the extraction of parabens (methylparaben, ethylparaben, and propylparaben) from six cosmetic samples (bodywash, deodorant, face cleanser, moisturizer, lotion, and toner) using UV-VIS spectroscopy. **Table 5** tabulates the relative recoveries of parabens from various cosmetic samples. For unspiked samples, the lowest amount of methylparaben was found in a lotion sample at 0.16 mg/L, while the highest amount was found in a face cleanser at 0.48 mg/L. The sample of a face cleanser had the lowest concentrations of ethylparaben and propylparaben, measuring 0.31 mg/L and 0.54 mg/L, respectively. Meanwhile, ethylparaben and propylparaben were detected in the greatest concentrations in the toner sample, with concentrations of 0.71 mg/L and 0.95 mg/L, respectively. Upon evaluation, the majority of the three paraben compounds found in the tested cosmetic samples were below the permitted range. According to Council Directive 76/78/EC of the European Community and the National Pharmaceutical Regulative Agency (NPRA), the maximum allowable concentration of methyl, ethyl, propyl, and butylparaben in cosmetic products is 0.4 % for a single ester and 0.8 % for an ester mixture [5]. Spiked recovery studies were run on six cosmetic products to further confirm the validity of the procedure. The cosmetic samples were spiked at 1.0 mg/L with three parabens (methylparaben, ethylparaben, and propylparaben) and analysed according to the

proposed procedure. The percentage recoveries for cosmetic samples spiked with 1.0 mg/L methylparaben were recorded in the range of 43.3 % to 64.6 %, with RSD values between 1.4 % and 4.0 %. Next, it was discovered that the extraction recoveries for cosmetic samples containing ethylparaben ranged from 51.7 % to 65.5 %, and the RSD values were between 1.5 % and 3.9 %. The six cosmetic samples were also spiked with 1.0 mg/L propylparaben, and the findings showed that it had the highest extraction recoveries, which ranged from 75.6 % to 113.3 %, and the RSD values were 1.9 % to 5.6 % when compared to methylparaben and ethylparaben. This result showed that the GMMIP produced had the highest selectivity and binding affinity to propylparaben. The excellent recognition of GMMIP for propylparaben is due to the presence of imprinted cavities of the GMMIP that hold the memory of size, shape, and functional groups of the propylparaben, allowing it to recognise the propylparaben specifically from its structural analogues, methylparaben and propylparaben. Therefore, it can be concluded that the proposed GMMIP extraction method was simple, effective, and cost-effective for its target molecules and their structural analogues.

Table 5. Relative recoveries of parabens from various cosmetic samples spiked to a concentration of 1 mg/L.

Cosmetic samples	Analyte: methylparaben		
	Found (mg/L)	Spiked with 1.0 mg/L methylparaben	
		Recovery (%)	Relative standard deviation (RSD)
Bodywash	0.47	44.3	3.4
Deodorant	Nd	62.1	2.4
Face cleanser	0.48	48.1	1.4
Moisturizer	0.24	64.6	4.0
Lotion	0.16	43.3	3.5
Toner	0.39	43.9	3.7

Cosmetic samples	Analyte: ethylparaben		
	Found (mg/L)	Spiked with 1.0 mg/L ethylparaben	
		Recovery (%)	Relative standard deviation (RSD)
Bodywash	0.60	56.4	2.8
Deodorant	0.45	61.7	1.5
Face cleanser	0.31	64.4	3.3
Moisturizer	0.50	51.7	2.5
Lotion	0.51	65.5	3.9
Toner	0.71	52.5	2.0

Cosmetic samples	Analyte: propylparaben		
	Found (mg/L)	Spiked with 1.0 mg/L propylparaben	
		Recovery (%)	Relative standard deviation (RSD)
Bodywash	0.62	85.2	5.4
Deodorant	0.55	93.6	4.5
Face cleanser	0.54	75.6	2.6
Moisturizer	0.74	113.3	3.9
Lotion	0.75	88.9	5.6
Toner	0.95	83.3	1.9

Keynotes: -

Nd: Not detected

3.3.3 Comparison of the proposed method with other methods

The magnetic molecular imprinting approach was compared with the earlier literature for the analysis of parabens in cosmetic samples, as listed in **Table 6**. To our knowledge, the developed method has never been used to determine and remove parabens from cosmetic samples. The GMMIP contains selective molecular recognition sites that can specifically bind parabens. The GMMIP preparation was environmentally friendly and appeared to be an efficient way to remove the propylparabens specifically from cosmetic samples with a good recovery of 75.6-113.3 %, and low values of LOD (0.03-0.05 mg/L) were obtained with some other methods. Additionally, due to the superior magnetic properties of the GMMIP, the developed method has an advantage over other methods in that it enables rapid separation and simple handling from the matrix using an external magnet. Thus, it simplifies and cuts down on the time required for pre-treatment procedures. Although the GMMIP has many of the advantages listed above, a key disadvantage is that, according to the selective assay, the result from real samples will be marginally impacted by the presence of structural analogues[65]. In conclusion, the

comparison demonstrated that the method used in this study for analyzing parabens in cosmetic samples was simple, feasible, and effective.

Table 6. Comparison of the analytical performance of the magnetic molecular imprinting technique with other methods for the determination of parabens in cosmetics.

Parabens	Sample matrix	Method/ Analytical instrument	Recovery (%)	LOD (mg/L)	Reference
MP, EP, PP, BP	After sun repair gel, hand cream, sunscreen, toner, whitening sunscreen lotion	SPE/CE	62.6-100.4	0.10-0.15	66
MP, EP, PP, BP	Cream, lotions	DLLME/ HPCE	71.1-112.6	0.2-0.375 mg/kg	67
MP, EP, PP, BzP	Cleanser, make-up remover, moisturizer, lotion, shower cream	CPE/HPLC-UV	68.0-112.0	0.01-0.02	53
BzP	Cosmetic and water samples	VA-DLLE/ UV-VIS	81.0-100.6	0.0476	40
MP, EP, PP, BzP	Cleansing water, facial cleanser, lotion, toning lotion	DLLME-MSPE/HPLC-UV	88.5-101	0.064-0.135	68
MP, EP, PP	Bodywash, deodorant, face cleanser, moisturizer, lotion, toner	Magnetic molecular imprinting technique/UV-VIS	43.3-113.3	0.03-0.05	This work

4. Conclusion

A novel green magnetic molecularly imprinted polymer (GMMIP) was successfully developed and evaluated for removing parabens from cosmetic products by using propylparaben as a template. The synthesis of green magnetic nanoparticles (MNP) via *Kesum* leaf extract and deep eutectic solvents (DES) were the green strategies that were introduced to further the idea of green chemistry. The synthesised GMMIP was characterised by FTIR, FESEM, and BET, and the resulting GMMIP exhibited an irregular spherical shape and was mesoporous with a pore size of 17.74 nm. The pH, kinetics, isotherms, and thermodynamics were also studied systematically. The propylparaben adsorption by GMMIP complied with the pseudo-second-order kinetic and Freundlich isotherm models at an optimum pH of 12. The thermodynamic results indicated that the adsorption process was physisorption, exothermic, spontaneous, and more favourable at 298 K. More significantly, the GMMIP offered an interesting method and was effectively used as an adsorbent to remove parabens from cosmetic samples. Due to the highly selective properties and rapid separation of the GMMIP extraction technique, it allows good recoveries of 75.6 % to 113.3 % for propylparaben compared to methylparaben and ethylparaben, with the limits of detection (LOD) and limits of quantification (LOQ) in the range of 0.03-0.05 mg/L and 0.11-0.16 mg/L, respectively. Therefore, it was underlined that the established method and the use of GMMIP as an adsorbent were efficient, simple, and cost-effective for the removal of parabens from cosmetic samples.

Conflict of interest

No conflict of interest in this study.

Acknowledgement

This work was supported by the Ministry of Higher Education (MOHE) through Fundamental Research Grant Scheme for Research Acculturation of Early Career Research (FRGS-Racer) RACER/1/2019/STG01/UTHM//2 Universiti Tun Hussein Onn Malaysia (UTHM) and Postgraduate Research Grant (GPPS) Vot H704.

References

1. Flasiński, M., Gawryś, M., Broniatowski, M., & Wydro, P. (**2016**). Studies on the interactions between parabens and lipid membrane components in monolayers at the air/aqueous solution interface. *Biochim. Biophys. Acta - Biomembr*, *1858*(4), 836-844.
2. Lincho, J., Martins, R. C., & Gomes, J. (**2021**). Paraben compounds—Part I: An overview of their characteristics, detection, and impacts. *Appl. Sci.*, *11*(5), 2307.
3. Alkafajy, S. A., & Abdul-Jabbar, R. A. (**2020**). Comprehensive effects of parabens in human physiology. *Ann Trop Med Public Health*, *23*, 23.
4. Hager, E., Chen, J., & Zhao, L. (**2022**). Minireview: Parabens Exposure and Breast Cancer. *Int. J. Environ. Res. Public Health.*, *19*(3), 1873.

5. Cabaleiro, N., De La Calle, I., Bendicho, C., & Lavilla, I. (**2014**). An overview of sample preparation for the determination of parabens in cosmetics. *TrAC - Trends Anal. Chem.*, *57*, 34-46.
6. Khesina, Z. B., Iartsev, S. D., Revelsky, A. I., & Buryak, A. K. (**2021**). Microextraction by packed sorbent optimized by statistical design of experiment as an approach to increase the sensitivity and selectivity of HPLC-UV determination of parabens in cosmetics. *J Pharm Biomed Anal.*, *195*, 113843.
7. Piao, C., Chen, L., & Wang, Y. (**2014**). A review of the extraction and chromatographic determination methods for the analysis of parabens. *J. Chromatogr. B Biomed. Appl.*, *969*, 139-148.
8. Cui, B., Liu, P., Liu, X., Liu, S., & Zhang, Z. (**2020**). Molecularly imprinted polymers for electrochemical detection and analysis: Progress and perspectives. *J. Mater. Res. Technol.*, *9*(6), 12568-12584.
9. Chen, L., Wang, X., Lu, W., Wu, X., & Li, J. (**2016**). Molecular imprinting: perspectives and applications. *Chem. Soc. Rev.*, *45*(8), 2137-2211.
10. López, A. S., Ramos, M. P., Herrero, R., & Vilariño, J. M. L. (**2020**). Synthesis of magnetic green nanoparticle–Molecular imprinted polymers with emerging contaminants templates. *J. Environ. Chem. Eng.*, *8*(4), 103889.
11. BelBruno, J. J. (2018). Molecularly imprinted polymers. *Chem. Rev.*, *119*(1), 94-119.
12. Liu, Y., & Dykstra, G. (**2022**). Recent progress on electrochemical (bio) sensors based on aptamer-molecularly imprinted polymer dual recognition. ***Sens.*** *Actuator A Phys.*, 100112.
13. Tabaraki, R., & Sadeghinejad, N. (**2020**). Preparation and application of magnetic molecularly imprinted polymers for rutin determination in green tea. *Chem. Pap.*, *74*(6), 1937-1944.
14. Yew, Y. P., Shameli, K., Miyake, M., Khairudin, N. B. B. A., Mohamad, S. E. B., Naiki, T., & Lee, K. X. (**2020**). Green biosynthesis of superparamagnetic magnetite Fe3O4 nanoparticles and biomedical applications in targeted anticancer drug delivery system: A review. *Arab. J. Chem.*, *13*(1), 2287-2308.
15. Macías-Martínez, B. I., Cortés-Hernández, D. A., Zugasti-Cruz, A., Cruz-Ortíz, B. R., & Múzquiz-Ramos, E. M. (**2016**). Heating ability and hemolysis test of magnetite nanoparticles obtained by a simple co-precipitation method. *J. Appl. Res. Technol.*, *14*(4), 239-244.
16. Ramesh, A. V., Rama Devi, D., Mohan Botsa, S., & Basavaiah, K. (**2018**). Facile green synthesis of Fe3O4 nanoparticles using aqueous leaf extract of Zanthoxylum armatum DC. for efficient adsorption of methylene blue. *J. Asian Ceram. Soc.*, *6*(2), 145-155.
17. Basavaiah, K., Kahsay, M. H., & RamaDevi, D. (**2018**). Green synthesis of magnetite nanoparticles using aqueous pod extract of Dolichos lablab L for an efficient adsorption of crystal violet. *Emerg. Mater. Res.*, *1*(3), 121-132.
18. Yew, Y. P., Shameli, K., Miyake, M., Kuwano, N., Bt Ahmad Khairudin, N. B., Bt Mohamad, S. E., & Lee, K. X. (**2016**). Green synthesis of magnetite (Fe3O4) nanoparticles using seaweed (Kappaphycus alvarezii) extract. *Nanoscale Res. Lett.*, *11*(1), 1-7.
19. Sirdeshpande, K. D., Sridhar, A., Cholkar, K. M., & Selvaraj, R. (**2018**). Structural characterization of mesoporous magnetite nanoparticles synthesized using the leaf extract of Calliandra haematocephala and their photocatalytic degradation of malachite green dye. *Appl. Nanosci.*, *8*(4), 675-683.
20. Kanagasubbulakshmi, S., & Kadirvelu, K. (**2017**). Green synthesis of iron oxide nanoparticles using Lagenaria siceraria and evaluation of its antimicrobial activity. *Def. Life Sci. J.*, *2*(4), 422-427.
21. Ridzuan, P. M., & Wan Salleh, W. (**2019**). Persicaria Odorata as a Potential Medicinal Plant-Mini Review. *J. nat. ayurvedic med.*, *3*(2), 1-4.
22. Abdul Aris, M. H., Lee, H. Y., Hussain, N., Ghazali, H., Nordin, W. N., & Mahyudin, N. A. (**2015**). Effect of Vietnamese coriander (Persicaria odorata), turmeric (Curcuma longa) and asam gelugor (Garcinia atroviridis) leaf on the microbiological quality of gulai tempoyak paste. *Int. Food Res. J.*, *22*(4).
23. Okonogi, S., Kheawfu, K., Holzer, W., Unger, F. M., Viernstein, H., & Mueller, M. (**2016**). Anti-inflammatory effects of compounds from Polygonum odoratum. *Nat. Prod. Commun.*, *11*(11), 1934578X1601101107.
24. Duan, H., Wang, D., & Li, Y. (**2015**). Green chemistry for nanoparticle synthesis. *Chem. Soc. Rev.*, *44*(16), 5778-5792.
25. Singh, P., Kim, Y. J., Zhang, D., & Yang, D. C. (**2016**). Biological synthesis of nanoparticles from plants and microorganisms. *Trends Biotechnol*, *34*(7), 588-599.
26. Li, X., & Row, K. H. (**2017**). Application of novel ternary deep eutectic solvents as a functional monomer in molecularly imprinted polymers for purification of levofloxacin. *J. Chromatogr. B Biomed. Appl.*, *1068*, 56-63.
27. Liu, Z., Wang, Y., Xu, F., Wei, X., Chen, J., Li, H., ... & Zhou, Y. (**2020**). A new magnetic molecularly imprinted polymer based on deep eutectic solvents as functional monomer and cross-linker for specific recognition of bovine hemoglobin. *Anal. Chim. Acta*, *1129*, 49-59.
28. Jablonský, M., Majová, V., Šima, J., Hroboňová, K., & Lomenová, A. (**2020**). Involvement of deep eutectic solvents in extraction by molecularly imprinted polymers—A minireview. *Xtal*, *10*(3), 217.
29. Lagashetty, A., & Ganiger, S. K. (**2019**). Synthesis, characterization and antibacterial study of Ag–Au Bi-metallic nanocomposite by bioreduction using piper betle leaf extract. *Heliyon*, *5*(12), e02794.
30. Belachew, N., Devi, D. R., & Basavaiah, K. (**2016**). Facile green synthesis of l-methionine capped magnetite nanoparticles for adsorption of pollutant Rhodamine B. *J. Mol. Liq.*, *224*, 713-720.
31. Ghasemzadeh, M. A., Abdollahi-Basir, M. H., & Babaei, M. (**2015**). Fe3O4@ SiO2–NH2 core-shell nanocomposite as an efficient and green catalyst for the multi-component synthesis of highly substituted chromeno [2, 3-b] pyridines in aqueous ethanol media. *Green Chem Lett Rev.*, *8*(3-4), 40-49.

32. Chen, D., Han, X., Wang, Q., Xie, L., Ai, Y., Dang, X., ... & Chen, H. (**2017**). Magnetic molecularly imprinted polymers for selective extraction and determination of naphthols. *Mikrochim. Acta*, *184*(9), 3373-3379.
33. Ma, W., Dai, Y., & Row, K. H. (**2018**). Molecular imprinted polymers based on magnetic chitosan with different deep eutectic solvent monomers for the selective separation of catechins in black tea. *Electrophor.*, *39*(15), 2039-2046.
34. He, Y., Tan, S., Abd EI-Aty, A. M., Hacımüftüoğlu, A., & She, Y. (**2019**). Magnetic molecularly imprinted polymers for the detection of aminopyralid in milk using dispersive solid-phase extraction. *RSC Adv.*, *9*(51), 29998-30006.
35. Pizan-Aquino, C., Wong, A., Aviles-Felix, L., Khan, S., Picasso, G., & Sotomayor, M. D. (**2020**). Evaluation of the performance of selective M-MIP to tetracycline using electrochemical and HPLC-UV method. *Mater. Chem. Phys.*, *245*, 122777.
36. Yusoff, M. M., Yahaya, N., Saleh, N. M., & Raoov, M. (**2018**). A study on the removal of propyl, butyl, and benzyl parabens via newly synthesised ionic liquid loaded magnetically confined polymeric mesoporous adsorbent. *RSC Adv.*, *8*(45), 25617-25635.
37. Tegegne, B., Chimuka, L., Chandravanshi, B. S., & Zewge, F. (**2021**). Molecularly imprinted polymer for adsorption of venlafaxine, albendazole, ciprofloxacin and norfloxacin in aqueous environment. *Sep. Sci. Technol.*, *56*(13), 2217-2231.
38. Omidi, F., Behbahani, M., Sadeghi Abandansari, H., Sedighi, A., & Shahtaheri, S. J. (**2014**). Application of molecular imprinted polymer nanoparticles as a selective solid phase extraction for preconcentration and trace determination of 2, 4-dichlorophenoxyacetic acid in the human urine and different water samples. *J. Environ. Health Sci. Eng.*, *12*(1), 1-10.
39. Saavedra, L. N. M., Penido, R. G., de Azevedo Santos, L., Ramalho, T. C., Baeta, B. E. L., Pereira, M. C., & da Silva, A. C. (**2018**). Molecularly imprinted polymers for selective adsorption of quinoline: theoretical and experimental studies. *RSC Adv.*, *8*(50), 28775-28786.
40. Beh, S. Y., Mahfut, I. W. B. D., Juber, N. I. B. M., Asman, S., Yusoff, F., & Saleh, N. M. (**2021**). Extraction of Parabens from Cosmetic and Environmental Water Samples Coupled With UV-Visible Spectroscopy. *J. Appl. Spectrosc.*, *87*(6), 1216-1223.
41. You, X., Piao, C., & Chen, L. (**2016**). Preparation of a magnetic molecularly imprinted polymer by atom-transfer radical polymerization for the extraction of parabens from fruit juices. *J. Sep. Sci.*, *39*(14), 2831-2838.
42. Dhar, P. K., Saha, P., Hasan, M. K., Amin, M. K., & Haque, M. R. (**2021**). Green synthesis of magnetite nanoparticles using Lathyrus sativus peel extract and evaluation of their catalytic activity. *Clean. Eng. Tech.*, *3*, 100117.
43. Eivazzadeh-Keihan, R., Radinekiyan, F., Maleki, A., Salimi Bani, M., & Azizi, M. (**2020**). A new generation of star polymer: magnetic aromatic polyamides with unique microscopic flower morphology and in vitro hyperthermia of cancer therapy. *J. Mater. Sci.*, *55*(1), 319-336.
44. Foroughirad, S., Arabzadeh, N., Mohammadi, A., & Khosravi, A. (**2018**). Synthesis and characterization of novel water-compatible magnetic molecularly imprinted polymer for tartrazine. *J. Chin. Adv. Mater. Soc.*, *6*(4), 706-721.
45. Amalia, S., Rafika, N. A., Hardiyanti, S. A., Ashari, A. D., Khabibi, B. W., Iftitah, E. D., ... & Sabarudin, A. (**2022**). Cobalt (II)-Mediated Molecularly Imprinted Polymer as a Monolithic Stationary Phase for Separation of Racemic Citronellal by Liquid Chromatography. *Sci. World J.*, *2022*.
46. Wang, D., Luo, X., Huang, Y., Wang, M., & Xia, Z. (**2020**). Combined magnetic molecularly imprinted polymers with a ternary deep eutectic solvent to purify baicalein from the Scutellaria baicalensis Georgi by magnetic separation. *Microchem. J.*, *157*, 105109.
47. Wang, J., Huyan, Y., Yang, Z., Zhang, H., Zhang, A., Kou, X., ... & Zhang, B. (**2019**). Preparation of surface protein imprinted thermosensitive polymer monolithic column and its specific adsorption for BSA. *Talanta*, *200*, 526-536.
48. Shahriman, M. S., Zain, N. N. M., Mohamad, S., Manan, N. S. A., Yaman, S. M., Asman, S., & Raoov, M. (**2018**). Polyaniline modified magnetic nanoparticles coated with dicationic ionic liquid for effective removal of rhodamine B (RB) from aqueous solution. *RSC Adv.*, *8*(58), 33180-33192.
49. Keluo, C., Tingshan, Z., Xiaohui, C., Yingjie, H., & Xing, L. (**2018**). Model construction of micro-pores in shale: A case study of Silurian Longmaxi Formation shale in Dianqianbei area, SW China. *Pet. Explor. Dev.*, *45*(3), 412–421.
50. Zhang, Y., Shao, D., Yan, J., Jia, X., Li, Y., Yu, P., & Zhang, T. (**2016**). The pore size distribution and its relationship with shale gas capacity in organic-rich mudstone of Wufeng-Longmaxi Formations, Sichuan Basin, China. *Nat. Gas Geosci.*, *1*(3), 213-220.
51. Angelov, T., Vlasenko, A., & Tashkov, W. (**2007**). HPLC determination of pKa of parabens and investigation on their lipophilicity parameters. *J. Liq. Chromatogr. Relat.*, *31*(2), 188-197.
52. Noorashikin, M. S., Mohamad, S., & Abas, M. R. (**2016**). Determination of parabens in water samples by cloud point extraction and aqueous two-phase extraction using high-performance liquid chromatography. ***Desalination Water Treat.***, *57*(47), 22353-22361.
53. Sohaimi, N. M., Saleh, N. M., Ariffin, M. M., Beh, S. Y., & Ahmad, R. (**2018**). An environmentally friendly method for extraction of parabens in various samples using low viscosity and low cloud point temperature surfactant. *Malaysian J. Anal. Sci.*, *22*(3), 365-374.
54. Asman, S., Mohamad, S., & Sarih, N. M. (**2016**). Study of the morphology and the adsorption behavior of molecularly imprinted polymers prepared by reversible addition-fragmentation chain transfer (RAFT) polymerization process based on two functionalized β-cyclodextrin as monomers. *J. Mol. Liq.*, *214*, 59-69.

55. Batool, F., Akbar, J., Iqbal, S., Noreen, S., & Bukhari, S. N. A. (**2018**). Study of isothermal, kinetic, and thermodynamic parameters for adsorption of cadmium: an overview of linear and nonlinear approach and error analysis. *Bioinorg. Chem. Appl.*, *2018*.
56. Kajjumba, G. W., Emik, S., Öngen, A., Özcan, H. K., & Aydın, S. (**2018**). Modelling of adsorption kinetic processes—errors, theory and application. *Adsorp Sci Technol.*, 1-19.
57. Tran, H. N., You, S. J., Hosseini-Bandegharaei, A., & Chao, H. P. (**2017**). Mistakes and inconsistencies regarding adsorption of contaminants from aqueous solutions: a critical review. *Water Res.*, *120*, 88-116.
58. Al-Ghouti, M. A., & Da'ana, D. A. (**2020**). Guidelines for the use and interpretation of adsorption isotherm models: A review. *J. Hazard. Mater.*, *393*, 122383.
59. Ayawei, N., Ebelegi, A. N., & Wankasi, D. (**2017**). Modelling and interpretation of adsorption isotherms. *J. Chem.*, *2017*.
60. Kecili, R., & Hussain, C. M. (**2018**). Mechanism of adsorption on nanomaterials. In *Nanomaterials in Chromatography.* Elsevier. (pp. 89-115).
61. Sahoo, T. R., & Prelot, B. (**2020**). Adsorption processes for the removal of contaminants from wastewater: the perspective role of nanomaterials and nanotechnology. In *Nanomaterials for the detection and removal of wastewater pollutant.* Elsevier. (pp. 161-222).
62. Inyinbor, A. A., Adekola, F. A., & Olatunji, G. A. (**2016**). Kinetics, isotherms and thermodynamic modeling of liquid phase adsorption of Rhodamine B dye onto Raphia hookerie fruit epicarp. *Water Resour. Ind.*, *15*, 14-27.
63. Húmpola, P. D., Odetti, H. S., Fertitta, A. E., & Vicente, J. L. (**2013**). Thermodynamic analysis of adsorption models of phenol in liquid phase on different activated carbons. *J. Chil. Chem. Soc.*, *58*(1), 1541-1544.
64. Egbosiuba, T. C., Abdulkareem, A. S., Kovo, A. S., Afolabi, E. A., Tijani, J. O., Auta, M., & Roos, W. D. (**2020**). Ultrasonic enhanced adsorption of methylene blue onto the optimized surface area of activated carbon: Adsorption isotherm, kinetics and thermodynamics. *Chem. Eng. Res. Des.*, *153*, 315-336.
65. Qin, D., Wang, J., Ge, C., & Lian, Z. (**2019**). Fast extraction of chloramphenicol from marine sediments by using magnetic molecularly imprinted nanoparticles. *Mikrochim. Acta.*, *186*(7), 1-10.
66. Ye, N., Shi, P., Li, J., & Wang, Q. (**2013**). Application of graphene as solid phase extraction absorbent for the determination of parabens in cosmetic products by capillary electrophoresis. *Anal. Lett.*, *46*(13), 1991-2000.
67. Xue, Y., Chen, N., Luo, C., Wang, X., & Sun, C. (**2013**). Simultaneous determination of seven preservatives in cosmetics by dispersive liquid–liquid microextraction coupled with high performance capillary electrophoresis. *Anal. Methods*, *5*(9), 2391-2397.
68. Gao, X., Xu, K., Chi, M., Li, J., Suo, L., Zhu, L., ... & Mu, J. (**2021**). Determination of four parabens in cosmetics by high-performance liquid chromatography with magnetic solid-phase and ionic dispersive liquid–liquid extraction. *Rev. Anal. Chem.*, *40*(1), 161-172.